

Magnetic acceleration of ultra-relativistic GRB and AGN jets

M. V. BARKOV^{1,2} AND S. S. KOMISSAROV,¹

¹ *Department of Applied Mathematics, The University of Leeds,
Leeds, LS2 9GT, UK*

² *Space Research Institute, 84/32 Profsoyuznaya Street,
Moscow, 117997, Russia*

E-mail: bmv@maths.leeds.ac.uk (MVB) and sergei@maths.leeds.ac.uk (SSK)

We present numerical simulations of cold, axisymmetric, magnetically driven relativistic outflows. The outflows are initially sub-Alfvénic and Poynting flux-dominated, with total-to-rest-mass energy flux ratio up to $\mu \sim 620$. To study the magnetic acceleration of jets we simulate flows confined within a funnel with rigid wall of prescribed shape, which we take to be $z \propto r^a$ (in cylindrical coordinates, with a ranging from 1 to 2). This allows us to eliminate the numerical dissipative effects induced by a free boundary with an ambient medium. We find that in all cases they converge to a steady state characterized by a spatially extended acceleration region. For the jet solutions the acceleration process is very efficient - on the outermost scale of the simulation more than half of the Poynting flux has been converted into kinetic energy flux, and the terminal Lorentz factor approached its maximum possible value ($\Gamma_\infty \simeq \mu$). The acceleration is accompanied by the collimation of magnetic field lines in excess of that dictated by the funnel shape. The numerical solutions are generally consistent with the semi-analytic self-similar jets solutions and the spatially extended acceleration observed in some astrophysical relativistic jets. In agreement with previous studies we also find that the acceleration is significantly less effective for wind solutions suggesting that pulsar winds may remain Poynting dominated when they reach the termination shock.

Keywords: jets acceleration; gamma-ray bursts; active galactic nuclei; pulsar wind nebulae.

1. Introduction

There is strong evidence for relativistic motions in jets that emanate from active galactic nuclei (AGNs). The Lorentz factors of blazar jets lie in the range $\sim 5 - 40$ [1–3].

In the case of AGNs there have indeed been indications from a growing body of data that the associated relativistic jets undergo the bulk of their acceleration on scales that are of the order of those probed by very-long-baseline radio interferometry. In particular, the absence of bulk-Comptonization spectral signatures in blazars has been used to infer that jet Lorentz factors ≥ 10 are only attained on scales $\geq 10^{17}$ cm [4].

The first theoretical clues to the necessity of relativistic motion in GRB's arose from the compactness problem [5]. The requirements that the source be optically thin can be used to obtain direct limits on the minimal Lorentz factor, $\Gamma \gtrsim 100$ [6, 7]. Recently, superluminal expansion was observed in the afterglow emission of GRB 030329 [8].

The main source of power of AGN and GRB jets is the rotational energy of the central black hole [9, 10] and/or its accretion disk. The naturally occurring low mass density and hence high magnetization of black-hole magnetospheres suggests that the rela-

tivistic jets originate directly from the black-hole ergosphere as Poynting-dominated outflows, whereas the disk surface launches a slower, possibly non-relativistic wind that surrounds and confines the highly relativistic flow. Although, dissipative processes may directly transfer the electromagnetic energy to emitting particles, the commonly held view is that it is first converted into the bulk kinetic energy and only subsequently channeled into radiation through shocks and other dissipative waves [11–16]. In the limit of ideal MHD such conversion can be achieved only via magnetic forces and the efficiency of this mechanism is the main subject of our investigation.

Since most of the acceleration takes place far away from the source the space-time is basically flat. We also use an isentropic equation of state $p = Q\rho^s$, where $Q = \text{const}$ and $s = 4/3$. Since we are interested in the magnetic acceleration of cold flows, we make Q very small, so the gas pressure is never a dynamical factor. This relation enables us to exclude the energy equation from the integrated system and overcome the stiffness of relativistic MHD in magnetically dominated regime.

Given the condition of axisymmetry the poloidal magnetic field is fully described by the so-called mag-

netic flux function $\Psi(r, z)$, the total magnetic flux enclosed by the axisymmetric loop circle $r, z = \text{const.}$ Moreover, for stationary flows there are 5 quantities that propagate unchanged along the magnetic field lines and thus are functions of Ψ alone. These are k , the rest-mass energy flux per unit magnetic flux; Ω , the angular velocity of magnetic field lines; l , the total angular momentum flux per unit rest-mass energy flux; μ , the total energy flux per unit rest-mass energy flux; and Q , the entropy per particle. For cold flows ($Q = 0, w = \rho c^2$) we have $k = \rho \Gamma v_p / B_p$, $\Omega r = v_p^{\hat{\phi}} - v_p B_p^{\hat{\phi}} / B_p$, $l = -I / 2\pi k c + r u^{\hat{\phi}}$, and $\mu = \Gamma(1 + \sigma)$, where Γ is the Lorentz factor, v_p is the magnitude of the poloidal velocity, B_p and $B_p^{\hat{\phi}}$ are the magnitudes of poloidal and azimuthal magnetic field, $I = c r B_p^{\hat{\phi}} / 2$ is the total electric current flowing through a loop of cylindrical radius r , σ is the ratio of the Poynting flux to the matter (kinetic plus rest-mass) energy flux, and $\Gamma \sigma = -\Omega I / 2\pi k c^3$ is the Poynting flux per unit rest-mass energy flux. It is easy to see that the Lorentz factor Γ cannot exceed μ .

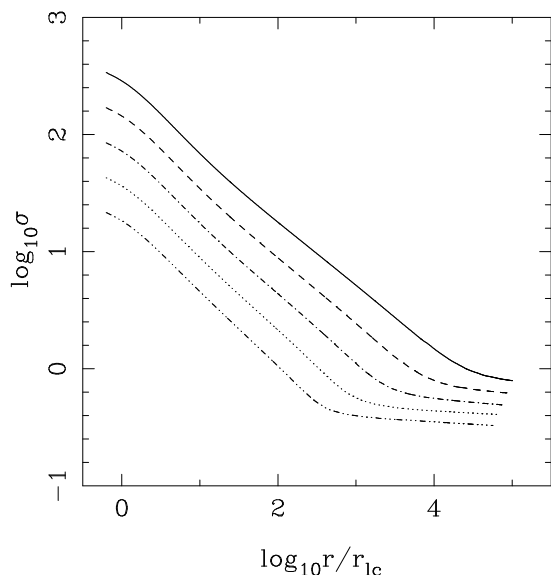


Fig. 1. Evolution of σ along the magnetic field line $\Psi = 0.8\Psi_{max}$ in models with $\sigma = 620$ (solid line), 310 (dashed line), 155 (dash-dotted line), 78 (dotted line) and 39 (dash-triple-dotted line).

2. Numerical Setup

In the simulation we deal with winds, or unconfined flows, and jets, or flows confined with a funnel. In

order to avoid complications due to numerical diffusion through the jet boundary we use solid funnels of paraboloidal shape, $z \propto r^a$, where z and r are the cylindrical coordinates.

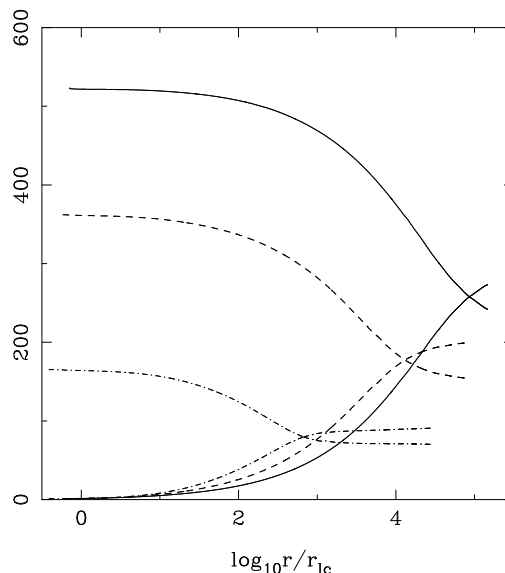


Fig. 2. $\Gamma \sigma$ (upper branch) and Γ (lower branch) along the magnetic field line $\Psi = 0.8\Psi_{max}$ (solid lines), along the magnetic field line $\Psi = 0.5\Psi_{max}$ (dashed lines), and along the magnetic field line $\Psi = 0.2\Psi_{max}$ (dash-dotted lines) in model $\sigma_0 = 620$.

The initial configuration corresponds to a non-rotating, purely poloidal magnetic field with approximately constant magnetic pressure across the funnel. The plasma density within the funnel is set to a small value so that the outflow generated at the inlet boundary can easily sweep it away. In order to speed this process up the longitudinal component of velocity inside the funnel and at the inlet is set to $0.7c$. In fact, we use the same type of initial and boundary conditions as described in our study of lower magnetization jets [16]. We constructed a grid of models with different funnel power geometry ($a = 1, 3/2, 2$) including unconfined wind, different initial magnetization ($\sigma = 10 \div 600$), and both solid and differential rotation at the base.

3. Results

Figure 1 shows the evolution of σ along the jet boundary for the models with $a = 3/2$, solid rotation, and the maximum magnetization at the base

$\sigma_0 = 39, 78, 155, 310$ and 620 (for solid rotation σ_0 increases with r). One can see that all solutions exhibit transition to the particle dominated regime ($\sigma < 1$). Prior to reaching the equipartition they are described by the same law $\sigma \propto (r/r_{lc})^{-3/5}$ and after this the evolution of σ slows down significantly. The dependence of ‘the equipartition’ radius r_{eq} on σ_0 can be approximated by

$$r_{eq} \simeq 0.079\sigma_0^{2.1}r_{lc} \text{ if } 10 < \sigma_0 < 620. \quad (1)$$

Figure 2 confirms similar evolution inside the jets. The normal pressure at the jet boundary is close to $p_n \propto R^{-2}$, where R is the spherical radius. In astrophysical conditions this pressure has to be balanced by the pressure of confining medium.

Figure 3 shows our results for the unconfined wind. One can see that magnetic acceleration in this case is much less effective in agreement with previous studies [17, 18].

4. Application to GRB and AGN Jets and PWN

The initial energy-to-mass flux ratio of jets in our simulations yields an upper limit on the terminal Lorentz factor $\Gamma_\infty = \mu$. In order to make further comparisons of our numerical models with observations we need to select suitable dimensional scales. The key scale in the problem of magnetic acceleration is the light cylinder (or the Alfvén surface) radius, r_{lc} . If the jets are launched by a rapidly rotating black hole in the center of an GRB or AGN then

$$r_{lc} \simeq 4r_g = 2 \times 10^6 (M/3 M_\odot) \text{ cm},$$

where $r_g \equiv GM/c^2$. In this estimate we assume that the angular velocity of the magnetic field lines is half of that of a maximally rotating (rotation parameter $a \simeq 1.0$) black hole. According to the results shown in equation (1), the jets enter the matter-dominated regime at a cylindrical radius

$$r_{eq} \simeq 5.9 \times 10^9 (\mu/150)^{2.1} (M/3 M_\odot) \text{ cm}.$$

The corresponding distance from the black hole is

$$R_{eq} \simeq 5.9 \times 10^{10} (\mu/150)^{2.1} (M/3 M_\odot) (0.1/\Theta_j) \text{ cm},$$

where Θ_j is the jet opening half-angle. Strong shock waves can appear only if $\sigma < 1$. For GRB jets, with $\mu \geq 150$ and $M \simeq 3 M_\odot$ this distance is remarkably close to the radius of Wolf-Raye stars. Thus,

in the collapsar scenario the conditions for development of strong fast shocks and associated gamma-ray emission are already satisfied when the jets break away from the progenitor star. The actual location of shocks, however, also depends on the scale of the central engine variability which puts it to larger distances.

Lower Lorentz factor of AGN jets imply lower magnetization parameter, $\mu \leq 30$. Combined with the black hole mass $M \simeq 10^8 M_\odot$ this gives $R_{eq} \simeq 2 \times 10^{17} \text{ cm}$ which is similar to the size of the ‘blazar zone’ inferred from the observations. Thus, the slow nature of magnetic acceleration of relativistic jets is in very good agreement with the observational constraints.

The velocity profile of jets with a solid body rotation at their base shows strong tangential discontinuity at the jet boundary which favors the photon-breeding mechanism of gamma-ray emission from AGN jets [19–21]. On the contrary, the gradual decline of Lorentz factor towards the jet boundary which we see in the models with differential rotation at the base significantly reduces its efficiency. This implies that gamma-ray observations can be used to determine whether the AGN jets originate directly from the black hole magnetospheres or from the magnetospheres of their accretion discs.

Like other researches [17, 18] we find that magnetic acceleration of highly magnetized unconfined winds is less ineffective. This is a rather uncomfortable conclusion since the successful MHD model of Pulsar Wind Nebulae [22–24] requires the pulsar wind to be particle dominated at the location of its termination shock. The two possible solutions to this problem suggested so far utilize the alternating structure of magnetic field in the wind from oblique rotators (‘striped wind’, [25]). Firstly, the alternating magnetic field can dissipate before reaching the termination shock, e.g. [26], with eventual conversion of the released heat into the bulk motion energy. Secondly, it can dissipate inside the shock layer of the termination shock itself [27]. In this case one cannot directly use the standard shock equations in order to determine the downstream state.

5. Conclusion

In validating the basic features of the simplified semi-analytic solutions, our numerical results go a long way toward establishing an ‘MHD acceleration and

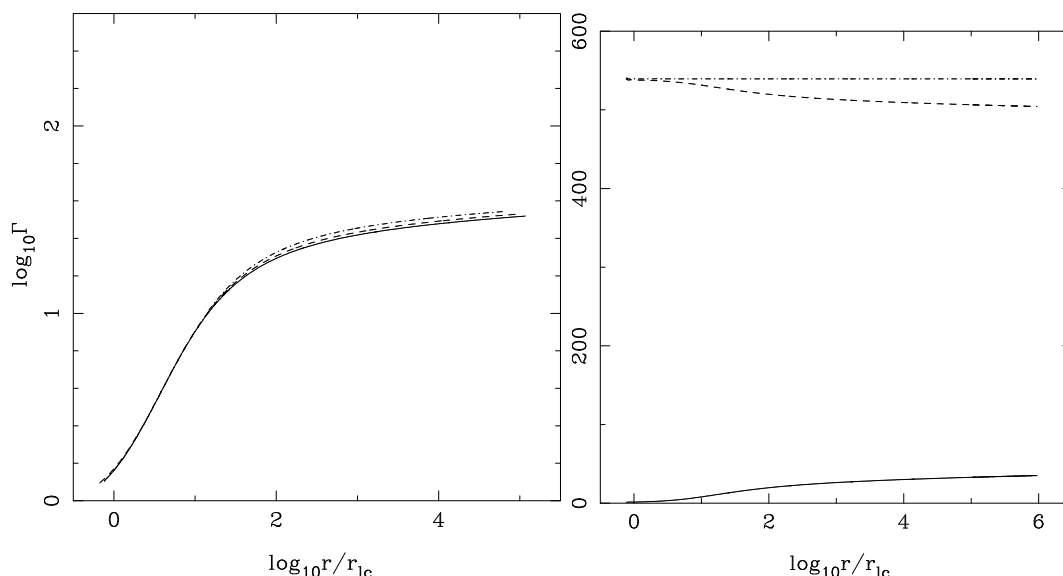


Fig. 3. Unconfined wind solution. Left panel: Lorentz factor along three different magnetic field lines: solid line - $\Psi = 0.8\Psi_{max}$, dashed line - $\Psi = 0.5\Psi_{max}$, dash-dotted line - $\Psi = 0.2\Psi_{max}$. Right panel: $\Gamma\sigma$ (solid line), μ (dashed line) and Γ (dash-dotted line) along the magnetic field line with $\Psi = 0.8\Psi_{max}$ as a function of cylindrical radius.

collimation paradigm” for relativistic astrophysical jets. In particular, they demonstrate that even jets with extremely high initial magnetization can be effectively accelerated via the ideal magnetic mechanism with more than a half of the Poynting flux converted into the bulk motion energy of the flows. The highest Lorentz factor reached in the simulations is $\Gamma = 300$ which is well within the range deduced for GRB jets. The slow character of magnetic acceleration allows dissipationless energy transport over large distances, the property which is deduced from observations and which is rather difficult to explain in other models of jet generation.

Interested reader can find more details about the method of our simulations and results for AGN jets in [16].

References

- [1] Cohen M. H. *et al.*, *ApJ*, **658**, 232, (2007).
- [2] Jorstad S. G. *et al.*, *AJ*, **130**, 1418, (2005).
- [3] Jorstad S. G. *et al.*, *ApJS*, **134**, 181, (2001).
- [4] Sikora M. *et al.*, *ApJ*, **625**, 72, (2005).
- [5] Rederman M., *Ann. N.Y. Acad. Sci.*, **262**, 164, (1975).
- [6] Krolik J.H. *et al.*, *ApJ*, **373**, 277, (1991).
- [7] Piran T., *Phys. Rep.*, **314**, 575, (1999).
- [8] Taylor G.B. *et al.*, *ApJ*, **609**, L1, (2004).
- [9] Blandford R. D. *et al.*, *MNRAS*, **179**, 433, (1977).
- [10] Lovelace R. V. E., *Nature*, **262**, 649, (1976).
- [11] Begelman M. C. *et al.*, *Reviews of Modern Physics*, **56**, 255, (1984).
- [12] Blandford R. D. *et al.*, *MNRAS*, **169**, 395, (1974).
- [13] Vlahakis N. *et al.*, *ApJ*, **596**, 1080, (2003a).
- [14] Vlahakis N. *et al.*, *ApJ*, **596**, 1104, (2003b).
- [15] Beskin V.S. *et al.*, *MNRAS*, **367**, 275, (2006).
- [16] Komissarov S. S. *et al.*, *MNRAS*, **380**, 51, (2007).
- [17] Beskin V.S. *et al.*, *MNRAS*, **299**, 341, (1998).
- [18] Bogovalov S. *et al.*, *MNRAS*, **305**, 211, (1999).
- [19] Aharonian F. *et al.*, *Science*, **314**, 1424, (2006).
- [20] Derishev E.V. *et al.*, *Physical Review D*, **68**, 043003, (2003).
- [21] Stern B.E. *et al.*, *MNRAS.tmp.1194S*, (2007).
- [22] Kenel C.F. *et al.*, *ApJ*, **283**, 694, (1984).
- [23] Komissarov S. S. *et al.*, *MNRAS*, **349**, 779, (2004).
- [24] Del Zana L. *et al.*, *A&A*, **421**, 1063, (2004).
- [25] Michel F. C., *Reviews of Modern Physics*, **54**, 1, (1982).
- [26] Arons J., *astro-ph/0710.1326B*, (2007).
- [27] Pétri J. *et al.*, *A&A*, **473**, 683, (2007).